

Mapping of low flip angles in magnetic resonance

Fabien Balezeau^{1*}, Pierre-Antoine Eliat², Alejandro Bordelois Cayamo³, Hervé Saint-Jalmes^{1,4}

¹ LTSI, Laboratoire Traitement du Signal et de l'Image INSERM : U642, Université de Rennes 1, Campus de Beaulieu, 263 Avenue du Général Leclerc - CS 74205 - 35042 Rennes Cedex, FR

² PRISM, Plate-forme Rennaise d'Imagerie et Spectroscopie Structurale et Métabolique IFR140, CEMAGREF, INRA, Université de Rennes 1, Biogenouest®, FR

³ Centro de Biofísica Médica Universidad de Oriente, Santiago de Cuba, CU

⁴ Centre Eugène Marquis CRLCC Eugène Marquis, Avenue Bataille Flandres-Dunkerque 35042 RENNES CEDEX, FR

* Correspondence should be addressed to: Fabien Balezeau <fabien.balezeau@gmail.com >

Abstract

Errors in the flip angle have to be corrected in many MRI applications, especially for T1 quantification. However, existing method of B1 mapping fail to measure lower values of flip angle despite the fact that these are extensively used in dynamic acquisition and 3D imaging. In this study, the nonlinearity of the radiofrequency transmit chain, especially for very low flip angles, is investigated and a simple method is proposed to determine accurately both the gain of the RF transmitter and the B1 field map for low flip angles. The method makes use of the Spoiled Gradient Echo sequence with long TR, such as applied in the double-angle method. It uses an image acquired with a flip angle of 90° as a reference image that is robust to B1 inhomogeneity. The ratio of the image at flip angle alpha to the image at flip angle 90° enables us to calculate the actual value of alpha. The present study was carried out at 1.5T and 4.7T, showing that the linearity of the radiofrequency supply system is highly dependent on the hardware. The method proposed here allows us to measure the flip angle from 1° to 60° with a maximal uncertainty of 10% and to correct T1 maps based on the variable flip angle method.

MESH Keywords Magnetic Resonance Imaging ; methods ; Monte Carlo Method ; Probability ; Radio Waves

Introduction

Knowledge of the actual flip angle and its spatial distribution is necessary in many MR applications, especially for T1 quantification (Venkatesan *et al* , 1998 ; Cheng *et al* , 2006 ; Deoni S, 2007 ; Treier *et al* , 2007 ; Schabel and Morrell, 2008). The problem has been well known since the early quantitative work on MRI, and many B1 mapping methods have subsequently been developed (Pelnar, 1986 ; Murphy-Boesch *et al*, 1987 ; Akoka *et al*, 1993 ; Insko and Bolinger, 1993 ; Stollberger and Wach, 1996 ; Cunningham *et al*, 2006 ; Dowell *et al*, 2007 ; Yarnykh, 2007 ; Morrell, 2008 ; Wang *et al*, 2009 ; Schär *et al*, 2010 ; Weber *et al*, 2010 ; Sacolick *et al*, 2010 ; Chang, 2011). Latest developments have mainly focused on *in vivo* imaging as well as accelerated sequences to enable 3D acquisition. The current trend is to perform rapid 3D flip angle mapping to correct 3D T1 maps calculated with the variable flip angle method (VFA). Studies on the optimization of the T1 measurement (Imran *et al*, 1999 ; Cheng *et al* , 2006 ; Deoni, 2007 ; Fleysher *et al* , 2007) have shown that low flip angles (20°) or even very low flip angles (<4°) are required when using VFA using the Spoiled Gradient (SPGR) echo sequence and short TR. However, none of the existing B1 mapping methods really lays emphasis on obtaining accuracy for low flip angle values. An analysis of existing methods (Morrell and Schabel, 2010) has shown that the performance of three of the most common methods is degraded, to different degrees, with decreasing flip angle. An additional restriction concerns all approaches based on a pair or set of proportional flip angles, such as applied in double-angle methods (Insko and Bolinger, 1993 ; Cunningham *et al* , 2006 ; Wang *et al* , 2009), the phase-sensitive method (Morrell GR, 2010) or the method of (Akoka, 1993) based on a stimulated echo: the radiofrequency supply system must be linear. If this condition is not satisfied, methods based on proportional flip angles become fundamentally flawed. Our study shows that the RF transmitters do not always provide the appropriate B1 field for a nominal flip angle, especially for the lowest flip angles. As a result, we propose a simple approach to determine both the gain of the RF transmitter and the spatial variations of the B1 field with a precision that does not decrease for low flip angles.

Materials and method

Characterization of the output RF pulse magnitude

The length, the magnitude and the shape of a radiofrequency pulse determine the flip angle of the magnetization. Generally, for a given sequence, the flip angle is proportional to the magnitude of the pulse. However, if the amplifier or other components of the RF supply system are used outside their range of linearity, this leads to significant bias in the resulting flip angle. Some effects of RF amplifier distortion on slice selection were studied by (Chan *et al* , 1992). To quantify the effect of this nonlinearity in commonly used pulses, we carried out direct measurements of the resulting pulse magnitude as a function of the nominal flip angle, at constant pulse length. A radiofrequency probe and oscilloscope (DSO6032A, Agilent Technologies) were used to register the waveform of the RF pulses and

measure their magnitude. Measurements were performed using two MR imaging systems: a whole-body Avanto 1.5T scanner (Siemens, Erlangen, Germany) using the body coil for transmission and a Bruker Biospec 4.7T scanner (Bruker Biospin, Rheinstetten, Germany) with a 36-mm linear volume coil for transmission. At 1.5T, 1-ms hermite pulses (Blümich, 2000) were registered for nominal flip angles of 1, 2, 3, 4, 8, 16, 32, 64 and 90°. At 4.7T, 1-ms sine cardinal pulses (Blümich, 2000) were registered for nominal flip angles of 1, 2, 3, 4, 5, 6, 8, 10, 12, 15, 20, 25, 30, 40, 50, 60, 70, 80 and 90°. The probe was placed at the centre of the receiver coil and all measurements falling outside the linearity range of the RF probe were discarded.

The Low Angle Mapping method

Our method is based on the same sequence used in the double-angle method: a SPGR sequence with a long TR (ideally $TR > 5T_1$), to obtain a flip angle weighting. The general expression of the SPGR sequence (Haase, 1990) is given by equation (1).

$$S = M_0 \frac{(1 - e^{-\frac{TR}{T_1}}) \cdot \sin \alpha}{1 - \cos \alpha \cdot e^{-\frac{TR}{T_1}}} e^{-\frac{TE}{T_2^*}}$$

(1)

With sequence parameters satisfying $TE < 5T_2^*$ and $TR > 5T_1$, the expression of the signal can be approximated by the equation (2). For low flip angles, the signal is poorly T1 weighted, thus the TR can be reduced. For example, at 10°, TR can be equal to T1 and at 1°, TR can be equal to 0.1T1.

$$S = M_0 \sin \alpha$$

(2)

Under the conditions of equation (2), the signal variations due to B1 inhomogeneity will be negligible if the flip angle is equal or close to 90°. Indeed, the signal variations between 82° and 98° do not exceed 1% of the 90° signal. In our approach, the signal of the image acquired with a 90° flip angle is considered independent of the flip angle, and is used as a reference value of M0. In other words, the 90° image provides a map of the other sources of inhomogeneity in the signal, arising from B0, M0 and the sensitivity of the receiver coil. By dividing the image at the nominal flip angle alpha by the 90° image, we obtain the sine of the actual flip angle alpha.

$$\alpha = \arcsin \frac{S_\alpha}{M_0} = \arcsin \frac{S_\alpha}{S_{90^\circ}}$$

(3)

The theoretical range of the method includes flip angles from 0° (excluded) to 90° (excluded), with a decreasing precision for flip angles close to 90°. However, the method is most advantageous when the flip angles are in the range from 1° to 20°, to the extent that the flip angle is equivalent to the ratio S_α/S_{90° . Considering that $S_\alpha \ll S_{90^\circ}$, the Angle to Noise Ratio of the flip angle map is equivalent to the Signal to Noise Ratio (SNR) of the image at flip angle alpha. Consequently, the method is able to map extremely low flip angles, despite the fact that because of the use of magnitude in signal processing, a non-zero mean value of the noise will appear and may be wrongly assigned to a signal value. Practically, this problem can be avoided by using a short TR at low flip angles and increasing the number of averages of the signal for the same total acquisition time. Thereby, even for very low flip angles, a good precision can be achieved without increasing the acquisition time.

Accuracy analysis

We used MATLAB (Mathworks, USA) to simulate the accuracy of the Low Angle Mapping (LAM) method and establish the main guidelines for using this approach. The three most important sources of errors were investigated: the actual effect of B1 inhomogeneity on the 90° reference image, the effect of the T1 weighting and the noise on the signal. Since the approximation of negligible effects of B1 on the 90° signal is a key assumption of the flip angle estimation, the effects of a bias on the 90° flip angle needs to be studied to determine the limits of the LAM. The method is symmetrical around 90°, so biases of +10° or -10° will result in the same flip angle map. We simulated actual flip angles of 70°, 75°, 80°, and 85° for the reference signal, instead of a nominal flip angle of 90°. Like the DAM, the residual T1 weighting is a source of error and cannot be totally avoided in conditions of *in vivo* acquisitions. For example, accurate B1 mapping in brain, while satisfying the condition $TR > 5T_1$, would need a TR of 10s. Finally, we characterized the precision of our method within its valid range by means of Monte Carlo simulations. The performances of the double-angle method and our method were simulated using an identical SNR. For both methods, we simulated 30 000 samples of the signal with an added Gaussian noise for 90 flip angle values from 1° to 90°. Then, the resulting flip angle samples and their probability density functions were calculated. The cross-comparison with other flip angle measurement methods is based on two studies (Wade and Rutt, 2007 ; Morrell and Schabel, 2010) analysing the efficiency of the best known methods: the Double-Angle Method (Insko and Bolinger, 1993), the phase sensitive method (Morrell, 2008) and Actual Flip-angle Imaging.

Experimental validation: B1 maps and application to T1 correction

Experimental validation was performed using the TO4 test-object (Spinsafety Ltd, Rennes, France). TO4 is a cylinder containing a CuSO_4 solution, which surrounds an assembly of 12 glass tubes filled with MnCl_2 solutions having T1 values ranging from 100 ms to 1000 ms. Both at 1.5T and 4.7T, T1 reference values of the test objects were obtained using several SE measurements, with chosen values of TR optimized for each tube (Spandonis *et al* , 2004). On the 1.5 T scanner, a set of SPGR images was acquired for B1 mapping with TR=2000 ms, TE=2.4 ms, alpha=[1 2 3 4 5 9 32 90]°, matrix size of 128x128, FOV 230 mm × 230 mm, 12 slices, slice thickness=5 mm; bandwidth= 55 000 Hz, 4 min 16 s imaging time per flip angle. Then, a set of SPGR 3D images for T1 mapping was acquired using the parameters: TR=6 ms, TE=2.4 ms, matrix size 256x256x48, alpha= [2 4 8 16 32 64]°. A 16-channels head coil was used as a receiver. On the 4.7T scanner, a set of SPGR images was acquired from one MnCl_2 tube of the TO4 assembly, with TR=800 ms, TE=2.4 ms, alpha=[3 4 5 8 9 10 12 16 17 25 30 60 90]°, bandwidth=50 000 Hz, matrix size=64x64, FOV=56 mm × 40 mm. T1 maps were drawn up with a SPGR sequence at TR=6ms, TE=2.4 ms alpha=[4 6 8 10 30 60 90]°, using the same geometry and bandwidth as the B1 maps. The 36mm volume coil was used for both transmitting and receiving. Images were processed using ImageJ (National Institute of Health, USA). Flip angles maps were calculated with LAM, and T1 maps were calculated with VFA firstly using the nominal flip angles and then the measured flip angles.

Results

RF measurement

Figure 1a shows the normalized output RF pulse magnitude as a function of the nominal flip angle for the 1.5T Siemens system, while Figure 1b shows this same function for the Bruker 4.7T system. Values are normalized as a fraction of the 90° magnitude. A constant value of 1 is expected for a perfectly linear RF transmitter. The transmitter of the Siemens system is linear in the range 5° to 90°. The transmitter of the Bruker system using the 36-mm volume coil for transmission is linear only for flip angles above 30°; flip angles lower than 4° were not registered because the measured signal was too low to be in the linearity range of the RF probe used. An alteration of the pulse shape is observed for low flip angles. Because of the limited dynamic range of the modulator, the lobes of the sinc pulses use on the 4.7T system disappear for flip angles lower than 30°.

Simulations of performance

Figure 2 shows the error on the flip angle estimation caused by different magnitudes of error in the 90° flip angle. An increase in the error on the 90° flip angle has two visible effects. At first, the maximal range of flip angle that can be measured is reduced by the absolute value of the error. The second effect is a systematic overestimation of the measured flip angle. An error of 5° has a negligible effect on the accuracy of the calculated flip angle. An error of 10° results in an overestimation of 1% for flip angles ranging from 1° to 50°. An error of 20° results in an overestimation of 7% for flip angles ranging from 1° to 30°.

Figure 3 shows the error on the flip angle estimation caused by a residual T1 weighting. The relative error does not depend on the flip angle measured. There is an overestimation of 15% of the actual flip angle value for TR=2T1 and 5% for TR=3T1, while the error is negligible for TR>5T1.

Figure 4 shows the probability density functions of the LAM and the DAM. While the precision of the double-angle method degrades for flip angles lower than 20°, the precision of our method is almost constant for flip angles ranging from 1° to 70° and degrades for flip angles higher than 70°.

Experimental B1 maps and T1 correction

The figure 5 shows flip angles measured with the Low Angle Mapping method versus nominal flip angles.

Figure 6 presents the flip angle map on the 1.5T Siemens system. The actual mean flip angle is 15% lower than the nominal flip angle, with a spatial variation of 0.2°.

Figure 7 presents corrected and uncorrected T1 maps of the TO4 test object. Reference T1 value of 380ms was obtained with optimized SE measurements for the CuSO_4 solution in the body of the test object.

Figure 8 presents the flip-angle map at 4.7T, for a nominal flip angle of 4° with a 36-mm volume coil. The actual flip angle determined with the LAM method is 5 times lower than the nominal flip angles. For very low flip angles, the nonlinearity of the transmitter is a predominant source of error in relation to the B1 inhomogeneity.

Figure 9 presents the uncorrected and corrected T1 maps calculated with VFA at TR=6 ms and flip angles of 4° and 30°. According to the SE reference measurements, T1 should be equal to 122 ms for the MnCl_2 tube. In this case, the flip-angle error leads to the measurement of a negative T1 value of -25 ms without correction. With correction, we obtain a measured mean value of 130 ms.

Discussion

Nonlinearity of the radiofrequency transmitter

Since the flip angle depends upon other parameters such as the pulse shape, the magnitude of the RF pulse is not a direct measurement of the flip angle. Yet, it gives a general idea on how the actual flip angles scales up with the nominal flip angles. RF measurements shown figure 1 are consistent with the flip angle values shown in figure 5, calculated using the LAM method. Our study shows that the nonlinearity of the RF transmitter can be sometimes a dominant factor of bias in T1 measurement, even more important than inhomogeneities of the B1 field due to the transmitting coil geometry or B1 penetration effects. When using very low flip angles, the problem of linearity can no longer be ignored. According to the comparison between two different systems, the accuracy of the flip angles is strongly dependent on the configuration of the system. On the 4.7T system, the same measurements repeated with a 72-mm transmitting coil produced similar results but for lower nominal angle values. We also observed a modification of the plot presented figure 1 when changing the pulse length. Thus, the calibration issue seems to be directly linked to the power delivered by the amplifier. As shown in Figs. 8 and 9, even with a relatively homogeneous B1 field, the mean value of the flip angle can be extremely different from the nominal value, which can make T1 measurements impossible. The nonlinearity observed for the 1.5T system is not considerable, but as shown figure 7, the lack of accuracy for very low flip angles can lead to non negligible errors in T1 mapping.

Guidelines and limits

The LAM method is based on the approximation that B1 inhomogeneities have a negligible effect on the signal at the 90° flip angle, and the conditions of validity of this assumption must be satisfied to obtain reliable flip angle measurements. In view of the simulations shown in Fig. 2, the LAM method is optimal if the spatial variation of the 90° pulse does not exceed $\pm 10^\circ$. Under these conditions, the error due to the approximation is negligible ($<3\%$) for flip angles of 1° to 70° . The method can still be used with spatial variations of the 90° pulse of $\pm 20^\circ$, with a 7% uncertainty on flip angles ranging from 1° to 30° . In our study, dielectric resonance effects were negligible. But at high field strength and in large objects, it may cause substantial B1 inhomogeneity in the 90° image.

The lowest flip angle that can be measured by the LAM method is determined solely by the SNR of the SPGR sequence at this flip angle. The measurement will be biased at very low SNR, if the noise distribution can no longer be considered as Gaussian. Since the number of excitations can be increased, and very short TR can be used for low flip angles there is no minimal angles value for our method.

The biased caused by incomplete relaxation can be problematic when dealing with long T1, typically in the brain or blood. For the 90° excitation, the complete relaxation is achieved when $TR > 5T1$, and we recommend choosing at least $TR > 3T1$. For lower flip angles, there is no analytical expression of the minimal TR to use. According to simulations $TR = 0.1 \cdot \alpha$ (in $^\circ$) is optimal for angles from 1° to 30° .

Comparison between the Low angle Mapping method and other B1 mapping approaches

Since the same sequence is used in the double-angle method, the comparison with Low Angle Mapping is straightforward. Both methods need the same acquisition time, so they differ only by their accuracy within the flip-angle range. The DAM is better for flip angles ranging from 50° to 90° , while both methods are equivalent in the range 35° to 50° and the LAM is better for flip angles ranging from 1° to 35° . Figure 4 shows a very good complementarity between the accuracy ranges of both methods. Based on the studies of (Wade and Rutt, 2007) and (Morrell and Schabel, 2010), we consider some other well known B1 mapping methods in our comparison. The phase sensitive method (Morrell, 2008) provides a good accuracy within a wider range than the DAM, yet the precision degrades for very low flip angles. However, by using a double angle, the method assumes the linearity of the flip angles. The Actual Flip Angle method (Yarnykh, 2007) has some advantages: linearity of the RF transmitter is not required and short TR are used, providing a better time-efficiency. But the method is not precise for low flip angles because the optimal ratio $TR2/TR1$ increases for lower flip angles, and the condition $TR2 \ll T1$ must be satisfied. The LAM is not really competitive with recently developed methods, if compared over the usual range of flip angles higher than 20° , but it fills a gap in the range of flip angles covered by existing methods.

In vivo-applications

According to the amount of quantitative studies using SPGR sequence with low flip angles, the method can be widely used for *in vivo* imaging in protocols involving T1 mapping and/or DCE MRI (Cheng *et al*, 2006; Deoni, 2007; Treier *et al*, 2007; Vautier *et al*, 2010; Schabel and Morrell, 2010). Most of publications on T1 mapping and DCE MRI that include a B1 correction finally never measure the actual value of the flip angles used in the sequence, and rely on a nominal B1 map. In contrast, our method is able to provide a direct measurement of the actual angle value for very low flip angles. For the 90° flip angles, the need to wait for the full recovery appears as a limitation for *in vivo* applications, especially for tissues with long T1. However, a small acquisition matrix (64x64) is generally sufficient to address both calibration and spatial variation issues. Moreover, parallel imaging method like GRAPPA or SENSE can be used, when available, to accelerate the acquisition of the 90° image. Since the problem of the linearity of the transmitter does not depend on the patient, it is possible to calibrate the flip angles once using test-objects, and to use another B1 mapping method to correct the inhomogeneity. However, the calibration depends on the configuration of the experiment i.e. the transmitting coil, the pulse width, the pulse shape. Therefore, the calibration would be required before each experiment but it would not provide information on the B1 map,

which depends on the subject and the geometry of the acquisition. Thus, an *in vivo* flip angle mapping is preferable for quantitative studies. We applied our method for whole body perfusion imaging experiments on mice. The B1 correction enables the quantification of the contrast agent on a wider field of view and with a better precision. The method was also tested on T1 mapping of the human brain. In both applications B1 maps were acquired in less than 10 min. The method can be implemented directly on every MRI system, and can be used without any notion of sequence programming.

Opportunities for improvement

Currently, the minimal TR used with the 90° flip angle limits the methods on its own to 2D acquisition, but for rapid *in vivo* 3D B1 mapping, time efficiency needs to be improved. Fortunately, most of the major improvements of the DAM, especially concerning time-efficiency, can be applied to the Low Angle mapping method. (Cunningham *et al* , 2006) proposed a saturation pulse to eliminate all T1 weighting. (Wang *et al* , 2009) used a catalysed SPGR sequence to compensate the T1 weighting while using a short TR. Lately, Wade (2009) developed the Double Angle Look Locker for accelerated 3D flip angle mapping. Using such accelerated sequences offers two major advantages. Firstly, reduced acquisition time is an obvious asset for *in vivo* imaging. Moreover, the possibility of performing 3D acquisitions instead of multislice 2D acquisitions reduces the error in B1 mapping caused by slice selection. Optimizing the time efficiency of Low Angle Mapping will be the subject of future studies.

Conclusion

This study has shown the need for a B1 mapping protocol that is able to measure the lowest flip angles and take into consideration possible nonlinearity of the RF supply system. We propose a very simple and straightforward method able to map accurately the lowest flip angles, assuming reasonable spatial inhomogeneity in the 90° pulse. Our method fully supplements the range of methods based on the double-angle approach and makes it possible to obtain excellent flip-angle accuracy at all values of flip angle.

Acknowledgements:

This work was supported by a financial grant from Region Bretagne. Dr M.S.N. Carpenter post-edited the English style.

References:

- Akoka S , Franconi FF , Seguin F , Le Pape A . 1993 ; Radiofrequency map of an NMR coil by imaging . *Magnetic Resonance Imaging* . 11 : 437 - 41
- Blümich B . 2000 ; NMR Imaging of materials .
- Chan F , Pauly J , Macovski A . 1992 ; Effects of RF amplifier distortion on selective excitation and their selection by prewarping . *Magnetic Resonance in Medicine* . 23 : 224 - 38
- Chang YV . 2011 ; Rapid B1 Mapping Using Orthogonal, Equal-Amplitude Radio-Frequency Pulses . *Magnetic Resonance in Medicine* .
- Cheng HLM , Wright GA . 2006 ; Rapid High-Resolution T1 Mapping by Variable Flip Angles: Accurate and Precise Measurements in the Presence of Radiofrequency Field Inhomogeneity . *Magnetic Resonance in Medicine* . 55 : 566 - 74
- Cunningham CH , Pauly J , Nayak KS . 2006 ; Saturated Double-Angle Method for Rapid B1+ Mapping . *Magnetic Resonance in Medicine* . 55 : 1326 - 33
- Deoni S . 2007 ; High-Resolution T1 Mapping of the Brain at 3T with Driven Equilibrium Single Pulse Observation of T1 with High-Speed Incorporation of RF Field Inhomogeneities (DESPO-T1-HIFI) . *Journal of Magnetic Resonance Imaging* . 26 : 1106 - 11
- Dowell NG , Tofts PS . 2007 ; Fast, Accurate, and Precise Mapping of the RF Field In Vivo Using the 180° . *Signal Null* . 58 : 622 - 30
- Fleysher L , Fleysher R , Liu S , Zaaoui W , Gonen O . 2007 ; Optimizing the Precision-Per-Unit-Time of Quantitative MR Metrics: Examples for T1, T2, and DTI . *Magnetic Resonance in Medicine* . 57 : 380 - 7
- Haase A . 1990 ; Snapshot FLASH MRI: applications to T, T, and chemical-shift imaging . *Magnetic Resonance in Medicine* . 13 : 77 - 89
- Imran J , Langevin F , Saint-James H . 1999 ; Two-points method for T1 estimation with optimized gradient-echo sequence. *Magnetic Resonance Imaging* . *Magnetic Resonance Imaging* . 17 : 1347 - 56
- Insko EK , Bolinger L . 1993 ; Mapping of the radiofrequency field . *Journal of Magnetic Resonance A* . 103 : 82 - 5
- Morrell GR . 2008 ; A Phase-Sensitive Method of Flip Angle Mapping . *Magnetic Resonance in Medicine* . 60 : 889 - 94
- Morrell GR , Schabel MC . 2010 ; An analysis of the accuracy of magnetic resonance flip angle measurement methods . *Physics in Medicine and Biology* . 55 : 6157 - 74
- Murphy-Boesch J , So GL , James TL . 1987 ; Precision mapping of the B1 field using the rotating-frame experiment . *Journal of Magnetic Resonance* . 73 : 293 - 303
- Pelnar J . 1986 ; Measurements of the distribution of B1 field in the presence of linear magnetic field gradient . *Journal of Magnetic Resonance* . 70 : 456 - 60
- Sacolick LI , Florian Wiesinger , Ileana Hancu , Vogel MW . 2010 ; B1 Mapping by Bloch-Siegert Shift . *Magnetic Resonance in Medicine* . 63 : 1315 - 22
- Schabel MC , Parker Dennis L . 2008 ; Uncertainty and bias in contrast concentration measurements using spoiled gradient echo pulse sequences . *Physics in Medicine and Biology* . 53 :
- Schabel MC , DiBella EVR , Jensen RL , Salzman KL . 2010 ; A model-constrained Monte Carlo method for blind arterial input function estimation in dynamic contrast-enhanced MRI: II. In vivo results . *Physics in Medicine and Biology* . 55 : 4807 - 23
- Schär M , Voncken EJ , Stuber M . 2010 ; Simultaneous B0- and B1+-Map Acquisition for Fast Localized Shim, Frequency, and RF Power Determination in the Heart at 3 T . *Magnetic Resonance in Medicine* . 63 : 419 - 26
- Spandonis Y , Heese FP , Hall LD . 2004 ; High resolution MRI relaxation measurements of water in the articular cartilage of the meniscectomized rat knee at 4.7 T . *Magnetic Resonance Imaging* . 22 : 943 - 51
- Stollberger R , Wach P . 1996 ; Imaging of the Active B1 Field In Vivo . *Magnetic Resonance in Medicine* . 35 : 246 - 51
- Treier R , Steingotter A , Fried M , Werner S , Boesiger P . 2007 ; Optimized and combined T1 and B1 mapping technique for fast and accurate T1 quantification in contrast enhanced abdominal MRI . *Magnetic Resonance in Medicine* . 57 : 568 - 76
- Vautier J , Heilmann M , Walczak C , Mispelter J , Volk A . 2010 ; 2D and 3D Radial Multi-Gradient-Echo DCE MRI in Murine Tumor Models With Dynamic R²-Corrected R1 Mapping . *Magnetic Resonance in Medicine* . 64 : 313 - 8
- Venkatesan R , Lin W , Haacke EM . 1998 ; Accurate Determination of Spin-Density and T1 in the Presence of RF-Field Inhomogeneities and Flip-Angle Miscalibration . *Magnetic Resonance in Medicine* . 40 : 592 - 602
- Wade T , Rutt B . 2007 ; Comparison of Current B1-mapping Techniques . *Proceedings of 15th ISMRM meeting* .
- Wade T , Rutt B . 2009 ; B1 correction using Double Angle Look-Locker (DALL) . *Proceedings of the International Society for Magnetic Resonance in Medicine 16th Scientific Meeting* .

- Wang D , Zuehlsdorff S , Larson AC . 2009 ; Rapid 3D radiofrequency field mapping using catalyzed double-angle method . NMR in Biomedicine . 22 : 882 - 90
- Weber H , Paul P , Elverfeldt DV , Hennig J , Zaitsev M . 2010 ; Extended Multi-Flip-Angle B1 Mapping: A 3D Mapping Method for Inhomogeneous B1 Fields . Concepts in Magnetic Resonance Part B (Magnetic Resonance Engineering) . 37B : 203 - 14
- Yarnykh VL . 2007 ; Actual Flip-Angle Imaging in the Pulsed Steady State: A Method for Rapid Three-Dimensional Mapping of the Transmitted Radiofrequency Field . Magnetic resonance in Medicine . 57 : 192 - 200

Figure 1

Normalized magnitudes of the radiofrequency pulse for flip angles ranging from 1° to 90°. (a) Bruker Biospec 4.7T, with a 36-mm inner diameter volume transmitting coil (b) Siemens Avanto 1.5T, with body transmitting coil

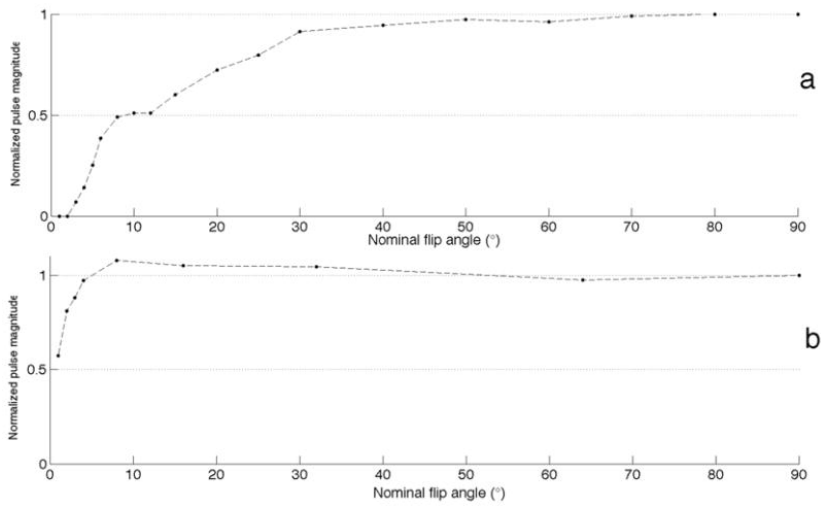


Figure 2

Bias on the estimated flip angle value due to inhomogeneity or systematic error of 5°, 10°, 15° and 20° in the 90°-flip angle

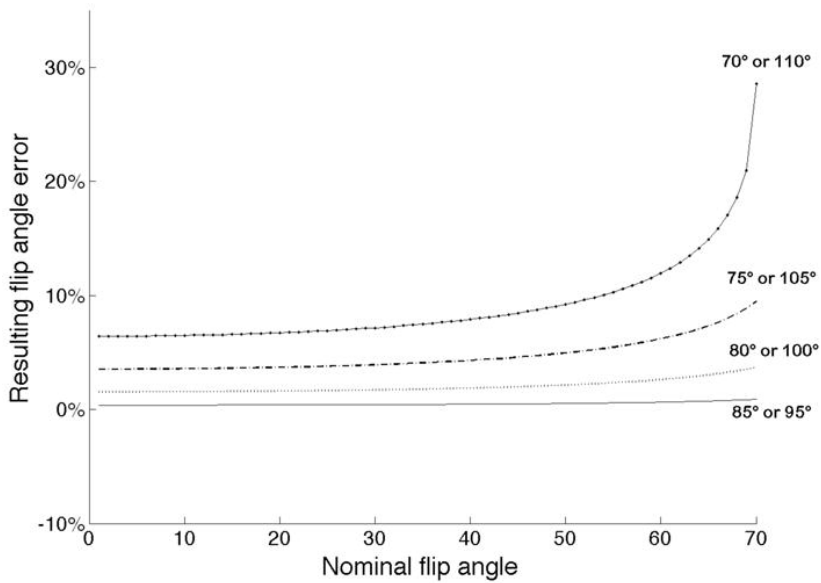


Figure 3

Error in the flip angle estimation caused by residual T1 weighting

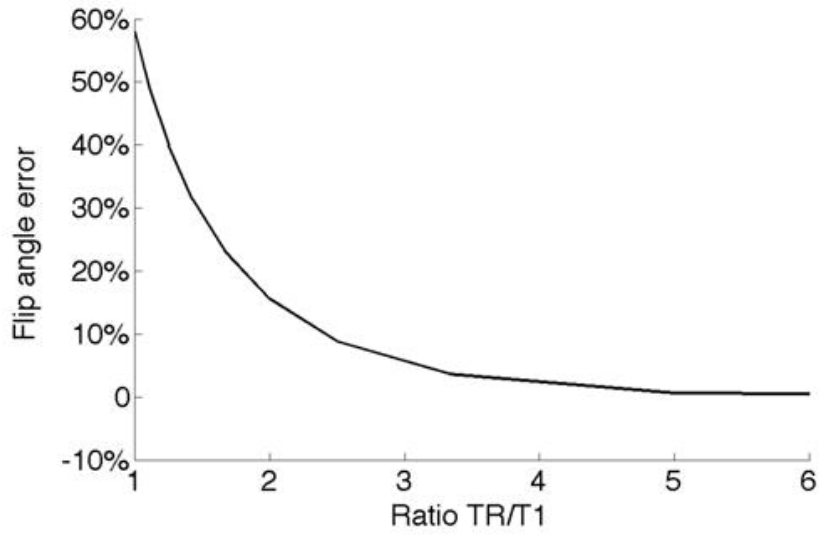


Figure 4

Monte-Carlo simulations of the probability density functions of our method and the double-angle method. At top, with SNR=100 for the 90° image. At bottom, with SNR=30 for the 90° image.

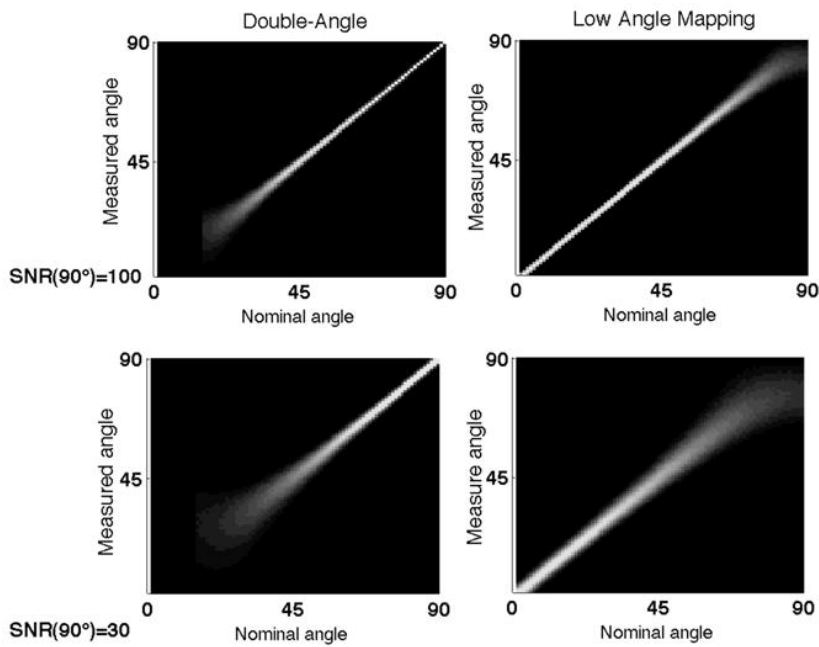


Figure 5

Flip angles measured with the low angle mapping method versus the nominal flip angles. a) on the Bruker 4.7T system and b) on the Siemens 1.5T system.

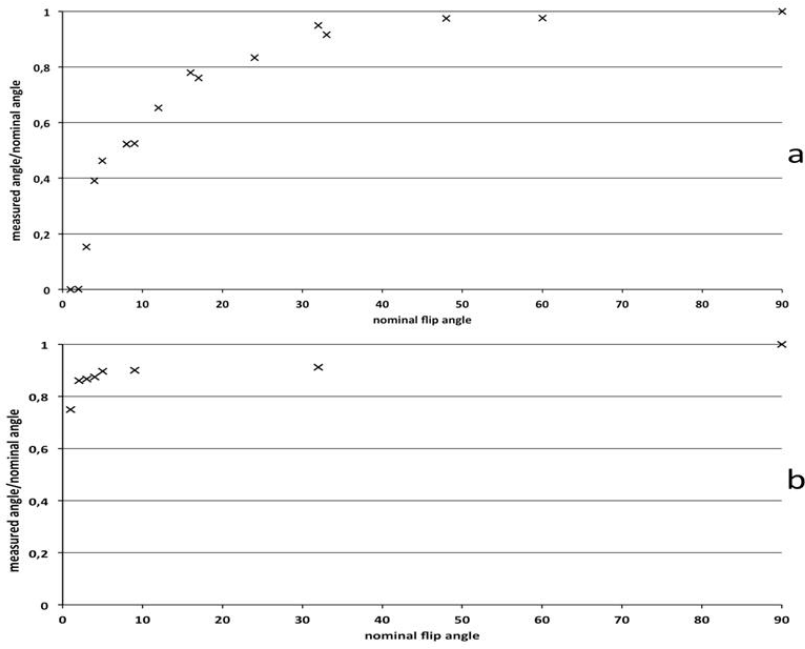


Figure 6

Flip angle map and corresponding cross-section in the TO4 test-object at 1.5T for a nominal flip angle of 2°

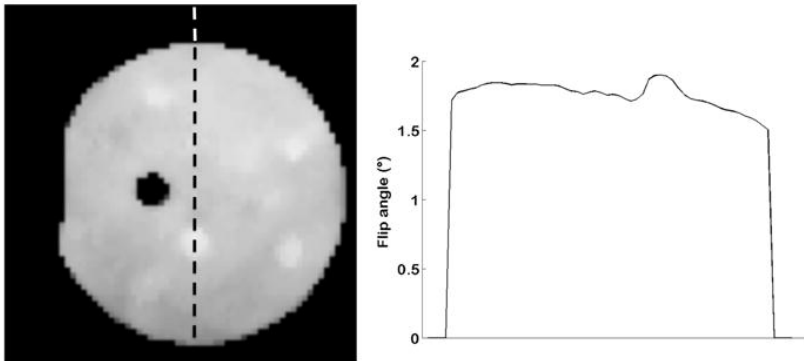


Figure 7

T1 maps of test-object using VFA (flip angles=[2,16]°, TR=6 ms) at 1.5T. (a) Uncorrected T1 map. (b) T1 map corrected with maps of both flip angles used. (c) Cross-section following the white dashed line on the uncorrected (dotted line) and corrected (solid line) T1 maps

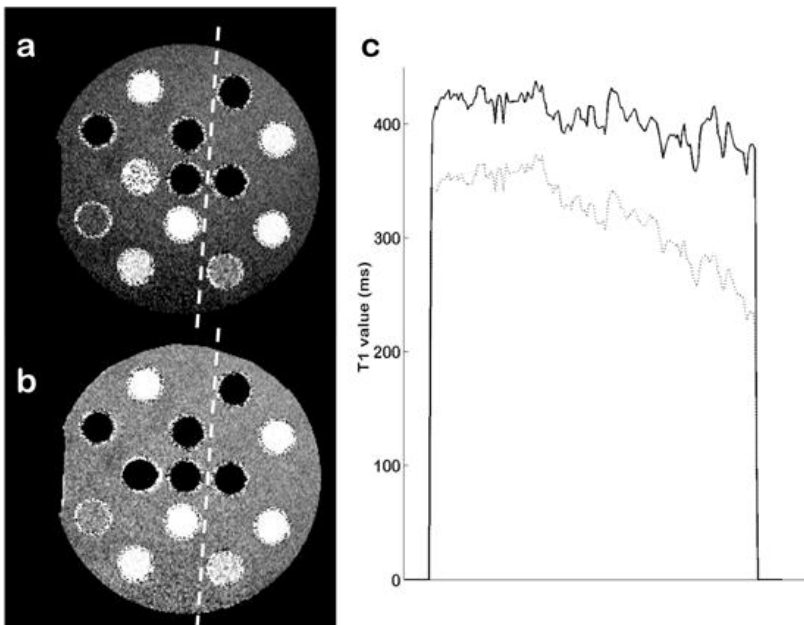


Figure 8

Flip-angle map and corresponding cross-section in the MnCl_2 tube at 4.7T for a nominal flip angle of 4°

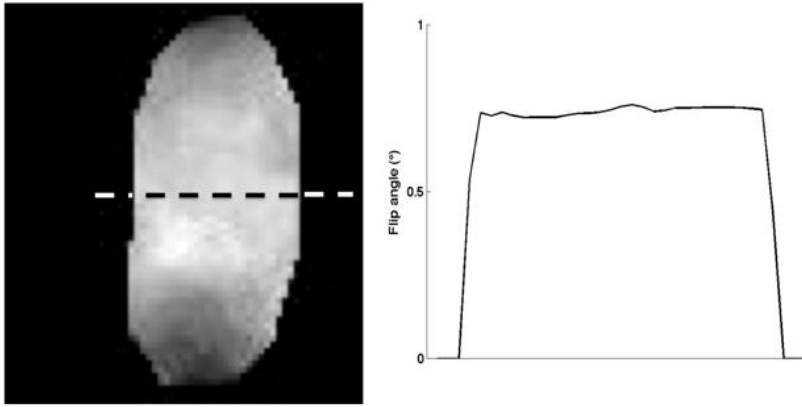


Figure 9

T1 maps of the tube MnCl_2 tube using VFA ($\alpha=[4, 30]^\circ$, $\text{TR}=6$ ms). (a) Uncorrected T1 map. (b) T1 map corrected with the flip angle map. (c) Cross-sections of uncorrected (dotted line) and corrected (solid line) T1 maps

